IEEE Access
Multidisciplinary | Rapid Review | Open Access Journal

Received March 3, 2022, accepted April 2, 2022, date of publication April 12, 2022, date of current version April 25, 2022.

Digital Object Identifier 10.1109/ACCESS.2022.3166918

A Multiobjective Approach for the Optimal Placement of Protection and Control Devices in Distribution Networks With Microgrids

CLEBERTON REIZ[1], (Graduate Student Member, IEEE), TAYENNE DIAS DE LIMA[1], (Graduate Student Member, IEEE), JONATAS BOAS LEITE[1], (Member, IEEE), MOHAMMAD SADEGH JAVADI[2], (Senior Member, IEEE), AND CLARA SOFIA GOUVEIA[2]

[1]Sao Paulo State University, Department of Electrical Engineering, Ilha Solteira 15385, Brazil
[2]Institute for Systems and Computer Engineering, Technology and Science, 4200-465 Porto, Portugal

Corresponding author: Cleberton Reiz (cleberton.reiz@unesp.br)

This work was supported in part by the Scholarship Granted from the Brazilian Federal Agency for Support and Evaluation of Graduate Education (CAPES), in the scope of the Program CAPES-PrInt, under Grant 88887.310463/2018-00, Mobility numbers 88887.569912/2020-00 and 88887.570741/2020-00; and in part by the São Paulo Research Foundation (FAPESP), under Grants 2015/21972-6, 2019/07436-5, and 2017/02831-8.

ABSTRACT Protection and control systems represent an essential part of distribution networks by ensuring the physical integrity of components and by improving system reliability. Protection devices isolate a portion of the network affected by a fault, while control devices reduce the number of de-energized loads by transferring loads to neighboring feeders. The integration of distributed generation has the potential to enhance the continuity of energy services through islanding operation during outage conditions. In this context, this study presents a multi-objective optimization approach for sizing and allocating protection and control devices in distribution networks with microgrids supplied by renewable energy sources. Reclosers, fuses, remote-controlled switches, and directional relays are considered in the formulation. Demand and generation uncertainties define the islanding operation and the load transfer possibilities. A non-dominated sorting genetic algorithm is applied in the solution of the allocation problem considering two conflicting objectives: cost of energy not supplied and equipment cost. The compromise programming is then performed to achieve the best solution from the Pareto front. The results show interesting setups for the protection system and viability of islanding operation.

INDEX TERMS Distribution systems, microgrids, protection system planning, non-dominated sorting genetic algorithm, compromise programming.

I. NOMENCLATURE

A. SETS AND INDICES

$\boldsymbol{\beta}$	Set of sections defined by reclosers and fuses.
$\boldsymbol{\delta}$	Set of sections defined by reclosers.
$\boldsymbol{\pi}$	Set of branches within each section.
$\boldsymbol{\sigma}$	Set of branches within each microgrid.
$\boldsymbol{\tau}$	Set of branches within each AS's transfer area.
$\boldsymbol{\Psi}$	Set of all devices installed.
$\boldsymbol{M}$, m	Set and index of microgrids.
$\boldsymbol{S}$, s	Set and index of scenarios.
$\boldsymbol{W}$, w	Set and index of ASs.
$\boldsymbol{Y}$, y	Set and index of the planning period.
f	Branch in short-circuit.
k	Type of device: 1, recloser; 2, fuse; 3, AS; 4 IID.
tc	Type of customer: residential R, commercial C, and industrial I.

B. VARIABLES AND FUNCTIONS

Cm_{ψ}	Annual maintenance cost of a device ψ.
$I^{t}_{i,y,s}$, $I^{p}_{i,y,s}$	Sum of section i and downstream loads during year y and scenario s for temporary and permanent faults, respectively.
$IOG_{i,y,s,m}$	Sum of loads within microgrid m in section i, year y and scenario s.
$IO_{i,y,s}$	Microgrids' loads in section i, year y, and scenario s.

The associate editor coordinating the review of this manuscript and approving it for publication was Arturo Conde.

n_k	Number of installed devices type k.
$S_{i,y,s}$	Sum of transferred loads downstream ASs within section i, year y, and scenario s.
$SW_{i,y,s,w}$	Sum of transferred loads downstream the AS w, within section i, year y, and scenario s.
T_y, P_y	ENS during temporary and permanent faults in the year y.

C. PARAMETERS

λ_h^t, λ_h^p	Failure rates of temporary and permanent faults per km year of the branch h.
Υ_k	Maximum number of devices type k.
Ca, Ci	Acquisition and installation costs.
IRR	Internal rate of return
L_h	Length of the branch h in km.
t_R^t, t_R^p	Time of power outage during temporary and permanent faults.
t_{Sw}	Time of power outage until the system's operator restoring the loads by using ASs.

II. INTRODUCTION

The traditional fault isolation and supply service restoration methods are essential for planning a distribution network to reach good reliability indices. Isolation methods include circuit breaker, reclosers and fuses action, while restoration methods comprise manual and automatic switches operation.

About 80% of faults occur in the distribution network, where approximately 75-90% are temporary in nature [1]. For this reason, reclosers play the important role of mitigating temporary failures in fast trip mode. If the fault becomes permanent, the recloser changes its operation mode, allowing fuses closer to the fault melt first, minimizing the impact on the system. Permanent faults, although less frequent, have a greater impact on the service interruption for customers, drastically increasing the amount of energy not supplied (ENS). During permanent faults, automatic switches (AS) available in the network could change their status by the system's operator and transfer part of the interrupted loads, into not faulted feeder sections, to neighbor feeders.

The integration of distributed generation (DG) brings several benefits and new challenges to distribution companies. A potential advantage is the islanding operation of DG units with part of the distribution network loads, operating as a microgrid [2]. However, the microgrid must have an adequate control system to guarantee the quality of energy supply to customers, in addition to safety when reconnecting with the distribution system. This strategy enables a substantial reduction in customer service interruptions during fault conditions. Therefore, the emergence of distribution systems with distributed generators and advanced autonomous systems offers a valuable opportunity to improve reliability through the islanding operation of microgrids [3], [4].

Several works consider the optimal allocation of protection and control devices without DG to improve the system reliability, [5]–[16]. In the last decade, the integration of DG units in distribution systems has grown exponentially, bringing several publications approaching the optimal allocation of protective devices in distribution networks with DG units [17]–[26]. However, just a few works consider the technical differences between dispatchable and renewable DG [23], [24], [26].

Some works consider the islanding operation [18]–[24], [26], while a few publications consider the demand and generation uncertainties to allow the operation of microgrids [26]. Most countries do not allow the DG islanding operation, despite the benefits that this technique can provide. The most common technical barriers comprise dual modes of operation, quality and control of energy, and problems of protection systems [2]. However, some papers in the literature have shown promising results in these topics [4], [20]–[24], [26]. Therefore, the islanding operation can be an attractive alternative to maximize the DG benefits and improve the distribution system's reliability.

A summary of the main features from specialized literature review is shown in Table 1. Protection and control include devices such as circuit breakers, reclosers, fuses, ASs, and island interconnection devices (IID). DG units are categorized as dispatchable (D) and renewable (R), where the second one depends on the power output uncertainties. The reliability indices considered in the literature review includes the cost of energy not supplied (CENS), system average interruption duration index (SAIDI), system average interruption frequency index (SAIFI), momentary average interruption frequency index (MAIFI), and the average system interruption duration index (ASIDI).

This work proposes an optimal allocation method of protection and control devices in distribution networks, considering the islanding operation and load transference possibility in a multi-objective approach. Unlike [5]–[8], [10]–[15], [17]–[21], this work includes DG units from different technologies.

Dispatchable DG units can easily operate in islanded mode, whereas renewable DG units, like photovoltaic (PV) and wind turbines (WT), depends on the associated uncertainties to provide the necessary power output to the load demand. In [26], the authors define the microgrid zone manually, considering a sum of total loads that can be easily supplied by the DG in island mode. In [23], the island operation using dispatchable or renewable DG units depends on the probability to generate power greater than or equal to a certain level. In [24], the island operation depends on the DG capacity and DG utilization, while [25] consider the DG capacity and voltage profile. However, evaluate the necessary energy during the island operation must be considered in renewable DG units to ensure a safer island operation since the associated uncertainties could provide lower power than the microgrid's demand, directly affecting the quality of energy supply and the microgrid's stability. The inclusion of batteries increases reliability in such conditions. Therefore, in contrast to [23]–[26], proper islanding operation in microgrids powered by renewable

TABLE 1. Main features from specialized literautre review.

Ref.	Scheme	Reliability indexes	Objective function	Protection and control devices				DG		BESS	Uncertainty			Island operation
				Recloser	Fuse	AS	IID	D	R		Load	Generation	SoC	
[5]	MILP	CENS	Single			✓								
[6]	MA	CENS	Single			✓								
[7]	MILP	SAIDI, SAIFI,	Single	✓	✓									
[8]	NLBP	SAIDI, SAIFI	Single	✓	✓									
[9]	MINLP	SAIDI, SAIFI	Single	✓	✓									
[10]	MINLP	SAIDI, CAIDI	Multiple	✓		✓								
[11]	MA	SAIDI, SAIFI	Multiple	✓		✓								
[12]	LP	CENS	Single	✓	✓	✓								
[13]	GA	SAIFI	Single	✓	✓	✓								
[14]	MACO	SAIDI, SAIFI	Multiple	✓	✓	✓								
[15]	MIP	CENS	Single	✓	✓	✓								
[16]	NSGA-II	SAIDI	Multiple	✓	✓	✓								
[17]	MILP	SAIDI, SAIFI, MAIFI, ASIDI	Multiple	✓		✓		✓						
[18]	GA	CENS	Single	✓				✓						✓
[19]	AA	CENS	Single	✓		✓		✓						✓
[20]	MTS	CENS	Multiple	✓	✓	✓	✓	✓						✓
[21]	NSGA-II	CENS	Multiple	✓	✓	✓	✓	✓						✓
[22]	GOA	CENS	Multiple	✓	✓	✓	✓	✓						✓
[23]	MINLP	CENS	Single	✓	✓	✓	✓	✓	✓					✓
[24]	MILP	SAIDI, MAIFI	Multiple	✓	✓	✓	✓	✓	✓					✓
[25]	NSGA-II	CENS, SAIDI	Multiple	✓	✓	✓	✓	✓	✓		✓	✓		✓
[26]	GA	CENS	Single	✓	✓	✓	✓	✓	✓		✓	✓		✓
PM	NSGA II	CENS	Multiple	✓	✓	✓	✓	✓	✓	✓	✓	✓	✓	✓

LP: Linear Programming; MIP: Mixed-Integer Programming; MILP: Mixed-Integer Linear Programming; NLBP: Nonlinear binary programming; MINLP: Mixed-Integer Nonlinear Programming; AA: Alliance Algorithm; GA: Genetic Algorithm; GOA: Genetic Algorithm with Steepest Descend Technique; NSGA-II: Non-dominated Sorting Genetic Algorithm II; MA: Memetic Algorithm; MACO: Multi-objective Ant Colony Optimization; MTS: Multi-objective Tabu Search; PM: Proposed method.

DG units is ensured by comparing the necessary energy during outage conditions and the available energy from all distributed energy sources within the microgrid, including battery energy storage systems (BESS). All issues mentioned above have not been simultaneously addressed yet.

The main contributions of this work are the following:

1) The sizing and allocation of all traditional protective and control devices: reclosers, fuses, and sectionalizing switches. The recloser's protection zone is expanded during temporary faults, increasing the reliability indices. Furthermore, the proposal considers the fuse-save scheme and load transference to neighbor feeders;
2) The use of dispatchable and renewable DG units, taking into account their power output uncertainties. For example, solar irradiation for PV units and wind speed for WT units. Generation and demand uncertainties are carried out using historical data classified by the k-means method;
3) The inclusion of IID to provide the possibility of islanded operation using DG units with part of distribution network loads as a microgrid. This strategy provides dual operation modes, allowing microgrids to change their status during temporary and permanent fault conditions. For microgrids supplied by intermittent generation, the islanded operation is strictly subject to the balance of energy available from distributed energy resources and microgrid's demand;
4) A fuzzy inference system (FIS) to estimate the batteries' state of charge (SoC) during the entire year. The fuzzy sets and fuzzy rules are adjusted using neural network tuning techniques. Associated uncertainties are used as input data, and the batteries' SoC from an optimal power flow model is considered output data. Also, a comparison is performed solving the allocation problem using batteries' SoC from both methods;
5) NSGA-II is implemented to solve the allocation problem of protective and control devices. The proposed method includes variable crossover and mutation rates and elitism strategy. NSGA-II generates efficient solutions while the compromise programming (CP) finds the best compromise solution among them, where the equipment cost and the CENS are the conflicting objectives.

III. METODOLOGY

In the problem for allocating protection and control devices, the best place to install each type of device is found by reducing outage impacts and equipment cost and by maximizing the reliability indices. Such devices have different behaviors and costs to mitigate faults.

A. PROTECTION DEVICES AND ISLAND OPERATION

Fuses are the most basic protective equipment in distribution networks. If a fault occurs downstream of a fuse, the high

short-circuit current flowing through the circuit heats the fuse link and causes it to melt, de-energizing downstream loads [20]. This type of equipment is helpful during permanent faults mainly because its low acquisition cost. However, fuses can also melt during temporary outages, unnecessarily de-energizing downstream customers. Therefore, reclosers play an important role in distribution networks with fuses by the fuse-save scheme. On the other hand, fuse-blow scheme melts the fuse first than reclosers' trip. Such technique reduces the MAIFI, but at the cost of increasing the SAIDI. The fuse-blow scheme is used in regions with high short-circuit currents, where the coordination cannot be realized.

A recloser is an AS with instantaneous and temporary over-current relays, ANSI 50/51, and a reclosing relay, ANSI 79. Instantaneous recloser's characteristic includes a predefined number of operations. The recloser opens the circuit to reduce the fault propagation during permanent faults, and the circuit remains opened until the maintenance team fix the problem. During temporary faults, the recloser's protective zone is expanded overlapping the protection zone of downstream fuses [21]. This scheme protects the fuse from melting during temporary faults.

Fig. 1 shows an example of a distribution system including a circuit breaker with reclosing function installed in branch 1 or B1, ASs in B19 and B88, a fuse in B32, and an IID in B37. If a fault occurs downstream of the fuse, the recloser in B1 will trip before the fuse melts. After a predefined sequence of operations, the recloser blocks the instantaneous function and operates slowly than the fuse, allowing it to melt first.

AS is used by the system's operator to isolate a fault or transfer loads to neighbor feeders. After the recloser's trip during a permanent fault within its protective zone, the system's operator can open the AS in B19 and close the AS in B88, transferring the loads to feeder 2 and reducing the number of disconnected customers.

IID is a bidirectional automatic recloser with reclosing function subjected to the synchronization verification [21]. This equipment is responsible to identify upstream faults and perform the microgrid's island operation. Dispatchable DG units can operate in island mode with voltage and frequency levels within limits set by regulatory agencies. Renewable DG units have their power output depending on the generation uncertainties. For instance, a PV unit with an adequate capacity could supply a microgrid if the solar irradiation provides sufficient power to the microgrid's loads. However, the associated uncertainties could provide lower power than the microgrid's demand, directly affecting the quality of energy supply and the microgrid's stability. Therefore, renewable DG units are not allowed to operate in islanded mode, except in cases of renewable DG with BESS, where its operation mode depends on the batteries' SoC.

B. UNCERTAINTY MODELLING

The growth of demand in distribution networks and its behavior during the year are uncertain. Renewable DG units also present uncertainties in their power output. Thus, based on [27], a set of scenarios for load demand, solar irradiation, wind speed, and SoC are generated from annual historical data of stochastic parameters to predict the hourly behavior throughout a year (8760 hours).

The estimation of batteries' SoC is based on the scenarios of demand, energy price, in addition to irradiation and wind speed due to PV and WT units, respectively. A fuzzy decision-making approach is proposed to achieve the SoC in each scenario. The fuzzy inference system (FIS) is shown in Fig. 2. Each input variable is represented by three triangular membership functions (MF).

The SoC from an entire year, obtained from the optimal power flow (OPF) model in [28], [29], is also used for tunning the FIS parameters using a neuro-fuzzy designer tool in MATLAB® environment [30]. Thus, 81 rules are created for the model structure considering the four inputs mentioned above. Besides, the output MF type is linear. Three days of each month are considered to train the FIS to reduce the computational response during the tuning process. Finally, the annual hourly SoC can be estimated and applied to the k-means method joint with the other parameters.

Fig. 3 shows the proposed structure process. Initially, all stochastic parameters are normalized, dividing each one by the maximum value. The annual historical data is divided into two seasons (time blocks), summer and winter, corresponding to the months April-September and October-March, in that order. Each time block presents two sub-blocks, day and night.

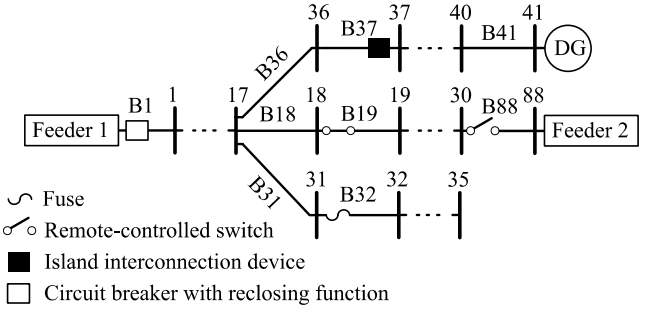

FIGURE 1. Example of an electrical distribution system.

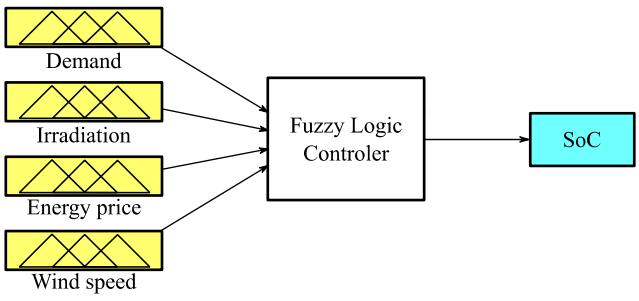

FIGURE 2. SoC estimation using a Fuzzy inference system.

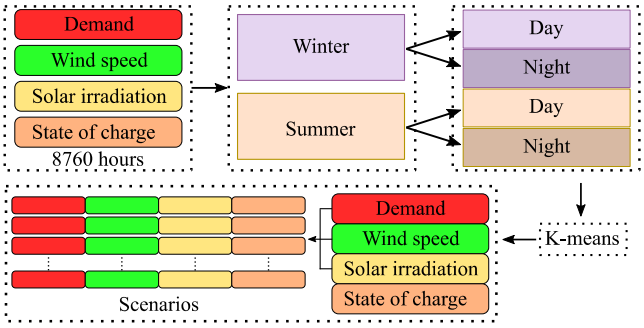

FIGURE 3. Scenario generation process.

The user must define the number of clusters. Each cluster represent a part of the stochastic parameters during the year. Thus, the k-means method is applied to each sub-block to reduce the stochastic parameters to the predetermined number of clusters [30]. As a result, the k-means method presents the centroids of each cluster. Finally, these centroids generate the set of scenarios.

C. OBJECTIVE FUNCTION AND CONSTRAINTS

The mathematical model comprises two conflicting objective functions (OFs), the CENS and costs of all protective and control devices (1). The equipment cost includes the acquisition, installation, and maintenance of each protective device.

$$Min\ \boldsymbol{OF}\ (f_1, f_2) = \left\{ C_{ENS} \quad C_{equipment} \right\} \tag{1}$$

The CENS in (2) is based on [21]. This OF evaluates the CENS considering for each year y of the set $\boldsymbol{Y}$. T_y and P_y can be estimated in (3) and (4), in that order. Section is defined as a set of branches and buses belonging to a device's protective zone. The sum of loads $I^t_{i,y,s}$, $I^p_{i,y,s}$, $IO_{i,y,s}$, and $S_{i,y,s}$ are previously multiplied by the demand factor in the scenario s. Functions in (5) and (6) are subjected to (7) and (8) in that order. Such constraints are related to cases of fault f within the microgrid zone and AS transfer area, respectively.

$$C_{ENS} = \sum_{tc\in\{R,C,I\}} Ce_{tc} \sum_{y\in Y} \frac{T_y + P_y}{(1+IRR)^y} \tag{2}$$

$$T_y = \sum_{s\in\boldsymbol{S}} \sum_{i\in\boldsymbol{\delta}} \sum_{h\in\boldsymbol{\pi}_i} (\lambda^p_h L_h t^t_R) \left[I^t_{i,y,s} - IO_{i,y,s} \right] \tag{3}$$

$$P_y = \sum_{s\in\boldsymbol{S}} \sum_{i\in\boldsymbol{\beta}} \sum_{h\in\boldsymbol{\pi}_i} (\lambda^p_h L_h) \left[\left(I^p_{i,y,s} - IO_{i,y,s} - S_{i,y,s} \right) t^p_R + S_{i,y,s} t_{Sw} \right] \tag{4}$$

$$IO_{i,y,s} = \sum_{m\in\boldsymbol{M}} IOG_{i,y,s,m} \tag{5}$$

$$S_{i,y,s} = \sum_{w\in\boldsymbol{W}} SW_{i,y,s,w} \tag{6}$$

$$IOG_{i,y,s,m} = 0, \quad f = h \forall h \in \boldsymbol{\sigma}_m \tag{7}$$

$$SW_{i,y,s,w} = 0, \quad f = h \forall h \in \boldsymbol{\tau}_w \tag{8}$$

The total equipment cost is calculated as given in (9), subjected to the amount of protection devices limited by the user, as shown in (10). The number of acquired and installed devices are represented by ω_1 and ω_2, in that order.

$$C_{equipment} = \sum_{i\in\omega_1} Ca_i + \sum_{i\in\omega_2} Ci_i + \sum\nolimits_{y\in Y} \sum\nolimits_{\psi\in\Psi} \frac{Cm_\psi}{(1+IRR)^y} \tag{9}$$

$$n_k \leq \Upsilon_k \tag{10}$$

Every solution must have a recloser in the first branch. Besides, fuses cannot be installed in the main feeder nor upstream reclosers and IIDs. Therefore, there is no bidirectional flow through these devices.

The proposed formulation is based on the following operation strategies:

1) IIDs are configured to act and isolate the microgrids first than reclosers during faults in the distribution network. This strategy guarantees the continuous supply of energy to the microgrid loads;
2) During faults inside the microgrid, the local protection sensibilizes first than other protection devices, disconnecting the DG units and sending a signal to open the switch at the PCC. This strategy improves system reliability by reducing the de-energized area;
3) Microgrids supplied by renewable DG can operate in islanded mode if the energy necessary in the i-th scenario plus the power losses are less than the energy available from distributed energy resources within the microgrid;
4) All pairs of protection devices are coordinated and have selectivity between them. Therefore, the fuse-blow scheme is an uninteresting solution, and it is not considered in this work.

D. COMPROMISE PROGRAMMING

The evaluation of both proposed OFs is achieved using the CP method, which is applied to solve simultaneously two objectives into a single OF [27]. Thus, the NSGA-II is proposed to achieve efficient non-dominated solutions.

The CP identifies the closest-to-ideal solutions through some distance measurement. These closest solutions are called compromise solutions and are formed from the non-dominated set, $\boldsymbol{\Omega}$, provided by NSGA-II method. Thus, the solution with the smallest length is presented to the decision-maker. Therefore, the CP seeks the compromise solution among the objectives of a multi-criteria decision-making problem.

The proposed OF in (1) must be normalized, as in (11), weighting the objectives according to their importance, where L_s is the distance metric.

$$Min\ L_s(x) = \sum_{j=1}^{K} (\alpha_j)^s \left(\frac{f_{j,max} - f_j(x)}{f_{j,max} - f_{j,min}} \right)^s, \quad \forall x \in \boldsymbol{\Omega}$$

$$\text{subject to: } 1 \leq s \leq \infty \quad \sum\nolimits_{j=1}^{K} \alpha_j = 1 \tag{11}$$

In (11), K is the number of objectives and α_j is the weighting factor for objective j, while $f_{j,max}$ and $f_{j,min}$ are the best and worst values of the j-th objective. The parameter s reflects the importance of the maximum deviation, while the parameter α_j reflects the relative importance of the j-th objective.

E. NSGA-II

The process of natural selection and evolution of species in nature is a consequence of a stochastic optimization process in a given environment and in real-time. GA is inspired by the natural selection process, where a chromosome represents a solution to the optimal allocation problem and its alleles represent the allocating of the protective devices on each branch of the distribution network [13]. Thus, the strongest individuals survive during the optimization process by transmitting to their descendants the best genes through genetic operators such as selection, crossover, and mutation.

An integer chromosome codification is considered, where the chromosome length depends on the number of distribution network branches. Numbers from one to four indicate the protection devices, while zero indicates no device allocated.

The selection stage consists of randomly choosing two pairs of individuals from a population P and comparing their quality (OF value). The best individual from each pair goes through the crossover process. In this stage, genetic material is exchanged between selected individuals. Genes are randomly mixed, creating a new pair of individuals that compose the new population. The crossover process is variable, randomly modifying the individual genes. The crossover rate, ρ_c, can vary according to (12). Such an approach prevents exploration restricted only to local solutions.

$$\rho_c = k^c_{max} - \frac{C^{SS}_i}{\eta_p}(k^c_{max} - k^c_{min}) \tag{12}$$

In (12), the number of similar solutions is represented by C^{SS}_i in the i-th generation, i.e., similar solutions concerning other population individuals, η_p, based on chromosome comparison. The adjustment factor k^c_{min} defines a minimum crossover rate to the GA process, while k^c_{max} is a maximum rate. Thus, the crossover process starts at high rates and decreases as the population loses its diversity. Before including the crossover individuals in the new population, the mutation process begins. The population mutation rate in (13) can also vary according to the same concept given in (12), where the superscript m is employed to represent the mutation parameters. Unlike the crossover process, the mutation rate increases as similar individuals in the population increase.

$$\rho_m = k^m_{min} - \frac{C^{SS}_i}{N}(k^m_{min} - k^m_{max}) \tag{13}$$

The elitism technique allows a more efficient exchange of genetic material between population individuals and is frequently applied in the specialized literature [13]. In the proposed methodology, elite solutions represent 1% of the current population. Such settings are updated every generation. GA runs until it reaches the stop criteria. Thus, the best solution is presented.

Generally, GA improves one or several objective functions using a function weighting system. In the second case, GA must run several times to find a set of efficient solutions [31]. Different from GA, NSGA-II can find a set of non-dominated solutions running once through a non-dominated sorting procedure for fitness assignments [32]. Crossover and mutation operators are the same in NSGA-II, while the selection operator presents additional procedures based on the non-dominance level and crowd distance between other solutions [33]. Fig. 4 shows the flowchart of the proposed methodology.

NSGA-II starts generating and evaluating a random population P_t, $t = 0$. Every evaluation process compares and stores the best fitness for each OF. Then, the offspring population Q_t is generated, evaluated, and combined with P_t into a single double-size population, R_t. The next step evaluates the dominance level of R_t using a counter, n_p. A non-dominated solution is not worse than others in all objectives and is better than others in at least one objective [32], presenting $n_p = 0$. All solutions not dominated by any other individuals are assigned to the best rank, front number 1, while other individuals are transferred to other frontiers according to their dominance level. Fig. 5 shows the non-dominated sorting procedure and the crowding distance sorting.

The population to the next generation is selected from R_t according to the frontier level, in ascending order. Since R_t is $2N$, the last frontier F_c to be included may not fit into the new population. Then, individuals from such front are

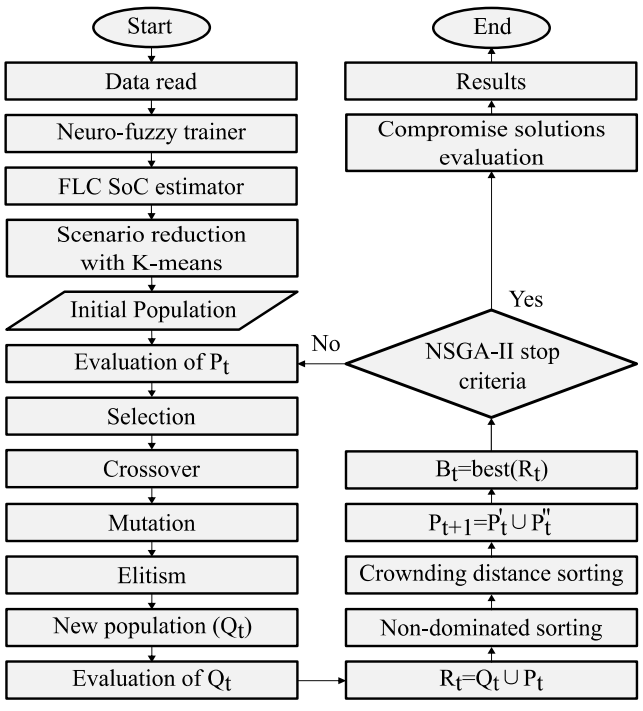

FIGURE 4. Flowchart of the proposed solution method.

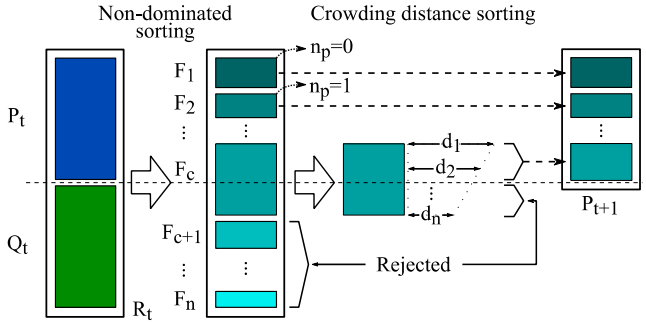

FIGURE 5. Non-dominated sorting procedure and th crowding distance sorting.

selected using the crowded-comparison operator in descending order, as shown in Fig. 5. The crowd distance is the Euclidian distance between neighbors in the same frontier, calculated as in (14), where $i+1$ and $i-1$ are the neighbors from solution i.

$$d_i = \sqrt{\sum_{k=1}^{p} \left(\frac{f_k^{i+1} - f_k^{i-1}}{\mathrm{f_k^{max}} - \mathrm{f_k^{min}}} \right)^2} \tag{14}$$

The OF k belongs to the OFs' set p. The crowded-comparison operator provides a good spread between solutions from the Pareto Front, promoting better options to the decision-maker.

Finally, the next iteration starts with the new population, and the process repeats until the algorithm reaches the stop criteria. In Fig. 4, P_t' contains all individuals from the $c-1$ best frontiers, and P_t'' contains the best solutions from the frontier F_c based on the crowded-comparison operator. The best fitness of each OF and the non-dominated solutions from the last population represent a compromise solution of the user-defined set $\mathbf{\Omega}$. Thus, the CP method evaluates this set and presents the best compromise solution to the decision-maker.

IV. NUMERICAL RESULTS

A 135-bus unbalanced distribution system has been employed to evaluate the proposed methodology, as shown in Fig. 6. This adapted network has 13.8 kV and 8.028 MVA. The planning horizon was established 20 years. Also, the demand increase is 2% per year, and the IRR is 5%. The recloser time is 0.01 hours for two reclosing shots in temporary faults (t_R^t). Thereafter, the instantaneous function is blocked. If necessary, the recloser trips again and takes 4 hours of average repair during permanent faults (t_R^p). The restoration time is 0.08 hours, which represents the time to the system operator control the necessary ASs and transfer loads to neighbor feeders (t_{Sw}). Each bus's demand consumption and ENS cost are divided as follows: 50% residential with \$1.5/kWh, 30% commercial with \$3/kWh, and 20% industrial with \$4.64/kWh. The equipment cost is shown in Table 2 [21].

TABLE 2. Costs of protection devices.

Devices	Current rate (A)	Acquisition costs (\$)	Instalation Costs (\$)	Maintenance Costs (\$)
Fuse	0-6	300	100	50
	6-10	400		
	10-15	500		
	15-25	600		
	25-40	700		
	40-65	800		
	65-100	900		
	100-140	1000		
	140-200	1100		
Automatic recloser	0-50	15000	2000	1000
	50-100	19000		
	100-300	22000		
	300-500	27000		
	500-1000	30000		
Automatic sectionalizing switch	0-50	3500	800	350
	50-100	4000		
	100-300	4500		
	300-500	5000		
	500-1000	5500		
IID	0-50	20000	2500	1500
	50-100	25000		
	100-300	30000		
	300-500	35000		
	500-1000	40000		

Five DG units are installed in the 135-bus system, where two are supplied by synchronous DG units (SG), two by photovoltaic panels, and one by a full-converter wind DG. Also, two BESS are installed near renewable DG units. BESS1 and BESS2 have 0.5 MW and 1 MW, respectively. SG units have 1.2 MVA capacity, while PV and WT units have 0.6 MVA. The power factor of dispatchable SG units is 0.92, while for PV and WT units, it is 0.98 and 0.90, respectively. Neighbor feeders 2 and 4 have 1.2 MW of available capacity, while feeders 3 and 5 have 0.75 MW. The power output calculation from PV and WT units considering associated uncertainties is based on [34].

Scenarios from solar irradiation and wind speed are taken from [35]. The set for load demand is taken from [36], and the energy price is taken from [37]. Protective devices are limited to 6 reclosers (R), 15 fuses (F), 4 AS, and 5 IID. The equipment cost of each device depends on its nominal current.

The proposed method is implemented in C++ general programming language due to its speed and computational efficiency.

A. CONVERGENCE CAPABILITY, TUNING PARAMETERS, AND RESULTS OVERVIEW

The convergence capability and tuning parameters of the proposed methodology are evaluated using the hypervolume metric [38]. The hypervolume indicator, HV, is a well-known method for assessing multi-objective optimizers. Such a method calculates the region enclosed by the Pareto Front solutions and a reference point. Usually, the reference point is the anti-ideal solution, i.e., the worst value from each objective function [39]. Posteriorly, HV is calculated by dividing

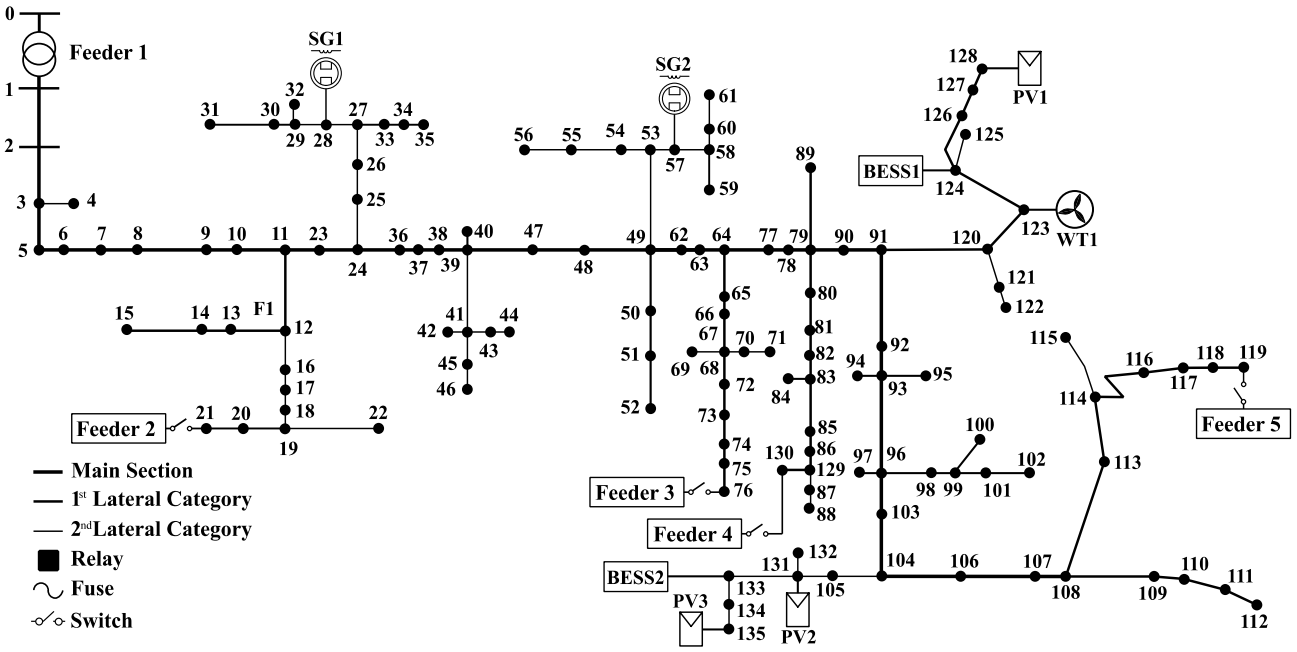

FIGURE 6. Distribution test system.

the region above Pareto Front solutions and the entire area, computed using the ideal solution and the reference point.

Fig. 7 shows the Pareto Front for different runs, each of them considering a different number of generations (G) and population size (P). The similarity between most Pareto Front solutions and the HV indicators highlights the proposed methodology's capability. Tests performed highlight that the number of generations and population size equal to or higher than 50 and 100, respectively, can achieve a HV higher than 0.85. The increase in the number of generational cycles and population size raises the HV. This value begins to stabilize for G and P greater than or equal to 200 and 1000.

The main differences between HVs are related to solver finding individuals with the lowest cost in one objective in contrast to other. For example, Run 6 presents a better HV regarding Run 5 because some solutions have lower equipment costs (see red circle). Thus, despite solutions in the middle of Pareto Front being better in Run 5, Run 6 presents slightly better HV using a lower population size.

Tests performed in this study have average computational times varying between 4 seconds (G10; P 100) and 14.5 minutes (G300; P1500). Computation times depends mainly on P and G values. Such time can take 30 minutes (G300; P1500) for tests which save all solutions found by the solver, as shown in Fig. 8.

The test with better hypervolume, Run 1, is chosen to detail in this section. Therefore, the number of generations and population is defined as 300 and 1500, respectively. Maximum and minimum mutation and recombination rates are defined before using the same technique, and their values are 0.9, 0.5, 0.1, and 0.025, in that order.

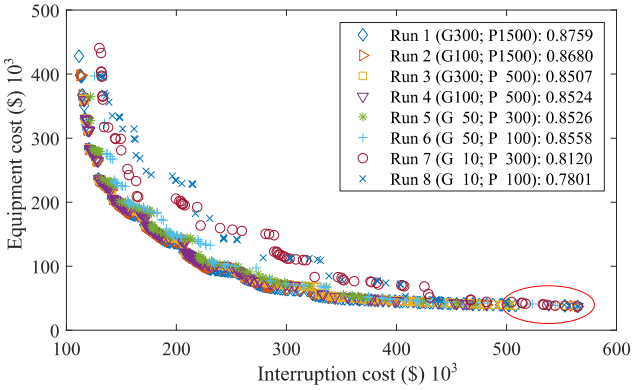

FIGURE 7. Pareto Fronts and their respective hypervolumes (HV).

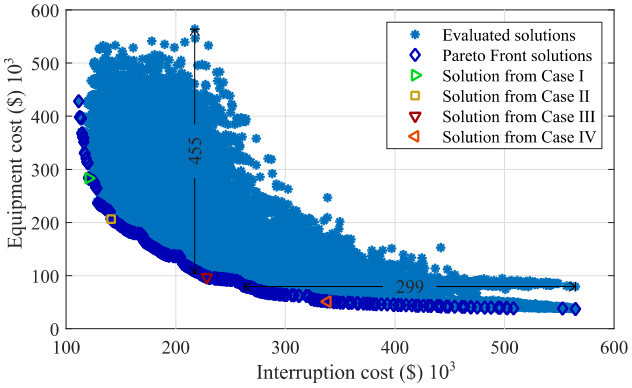

FIGURE 8. Solutions found by NSGA-II.

All solutions found by NSGA-II are shown in Fig. 8. Solutions highlighted in dark blue represent the set $\boldsymbol{\Omega}$ or Pareto Front between both objectives CENS and equipment cost. Such a set includes 300 non-dominated solutions. Colors green, yellow, red, and orange represent the studied cases I, II, III, and IV, in that order, also belonging to the Pareto Front. Other individuals, highlighted in light blue, were evaluated during the resolution process.

Solutions with similar equipment costs can reach a CENS difference of around \$299,000, while solutions with similar CENS can reach an equipment cost difference of \$455,000, as shown in Fig. 8. Maximum and minimum values from CENS and equipment cost are \$564,684, \$111,483, \$428,057, and \$37,085. The individual with the highest CENS is also a non-dominated solution. Such individual has merely the substation protection, R1. On the other hand, the individual with the highest equipment cost is dominated by other solutions. The cost of each control or protective device depends on the nominal current. Therefore, solutions with higher equipment costs include the maximum number of devices allowed and are installed in branches with higher current flow.

Fig. 9 shows a comparison of Pareto Front solutions based on the number of protection and control devices. The first individual has the highest CENS value from left to right, while the last one has the lower value. All solutions have a reclosing relay in the substation due to restrictions imposed on such equipment. 61% includes more than one recloser. Solutions with at least one fuse represent 99.67% of Pareto Front individuals, while 13% include the maximum allowed number. ASs are present in 80.33% of solutions, with 26,67% including the maximum permitted limit. IIDs have minor participation in the entire set, with 44% of solutions with at least one device installed. Only 4% of solutions include four IID. The same behavior is observed in reclosers, where only 6.33% of Pareto Front solutions consider four or more of such devices. Reclosers can reduce large amounts of ENS, but its costs have low attractiveness from the equipment cost point of view.

Individuals with two reclosers represent 46.33% of Pareto Front solutions, while cases with three reclosers represent 8.33%. Companies usually recommend up to 3 devices in series due to the difficulties imposed when defining how to coordinate such equipment. Therefore, the associated high cost naturally avoids solutions with many reclosers in series.

Fuses and ASs are the most attractive options for the proposed methodology. Many IIDs can be allocated when ENS reduction is more relevant than the costs involved.

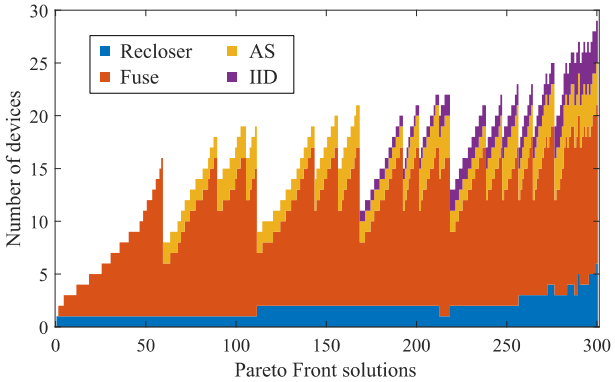

FIGURE 9. Pareto front solutions with the CENS in descending order.

B. STUDY CASES CONSIDERING SOC SCENARIOS FROM OPF MODEL

Different scenarios are evaluated to show how the decision-maker preferences influence the most appropriate solution produced by the proposed approach. Such methods are defined by changing each OF's weighting factor in the compromise programming. Thus, four compromise solutions are evaluated as follows:

I) CP with a high emphasis on the CENS, i.e., $\alpha_1 = 0.9$ and $\alpha_2 = 0.1$;
II) The CP emphasizing the CENS, $\alpha_1 = 0.7$ and $\alpha_2 = 0.3$;
III) OFs with the same weighting factor, $\alpha_j = 0.5, \forall j$;
IV) The CP focusing on the equipment cost, $\alpha_1 = 0.2$ and $\alpha_2 = 0.8$.

Table 3 shows the cost of all protective and control devices installed in each case study. Also, Fig. 10 shows the compact test system with all protection devices allocated for each case.

The low cost of fuses encourages their installation in large quantities in most solutions of Pareto Front. Fuses allocation by the method occurred even on lines with low load, such

TABLE 3. Size of each devices in all case studies.

Case I							
DP	**I (A)**	**DP**	**I (A)**	**DP**	**I (A)**	**DP**	**I (A)**
R1	100-300	**AS2**	0-50	**F4**	6	**F10**	10
R2	0-50	**AS3**	0-50	**F5**	40	**F11**	10
R3	0-50	**AS4**	0-50	**F6**	40	**F12**	10
IID1	0-50	**F1**	6	**F7**	65	**F13**	25
IID2	0-50	**F2**	15	**F8**	10	**F14**	15
IID3	0-50	**F3**	25	**F9**	100	**F15**	40
AS1	0-50						
Case II							
DP	**I (A)**	**DP**	**I (A)**	**DP**	**I (A)**	**DP**	**I (A)**
R1	100-300	**AS3**	0-50	**F5**	40	**F11**	10
R2	0-50	**AS4**	0-50	**F6**	40	**F12**	10
IID1	0-50	**F1**	6	**F7**	65	**F13**	25
IID2	0-50	**F2**	15	**F8**	10	**F14**	15
AS1	0-50	**F3**	25	**F9**	100	**F15**	40
AS2	0-50	**F4**	6	**F10**	10		
Case III							
DP	**I (A)**	**DP**	**I (A)**	**DP**	**I (A)**	**DP**	**I (A)**
R1	100-300	**F1**	6	**F4**	40	**F7**	65
R2	0-50	**F2**	6	**F5**	65	**F8**	25
AS1	0-50	**F3**	40	**F6**	100	**F9**	40
AS2	0-50						
Case IV							
DP	**I (A)**	**DP**	**I (A)**	**DP**	**I (A)**	**DP**	**I (A)**
R1	100-300	**F3**	6	**F6**	65	**F9**	65
F1	6	**F4**	40	**F7**	100	**F10**	25
F2	65	**F5**	40	**F8**	10	**F11**	40

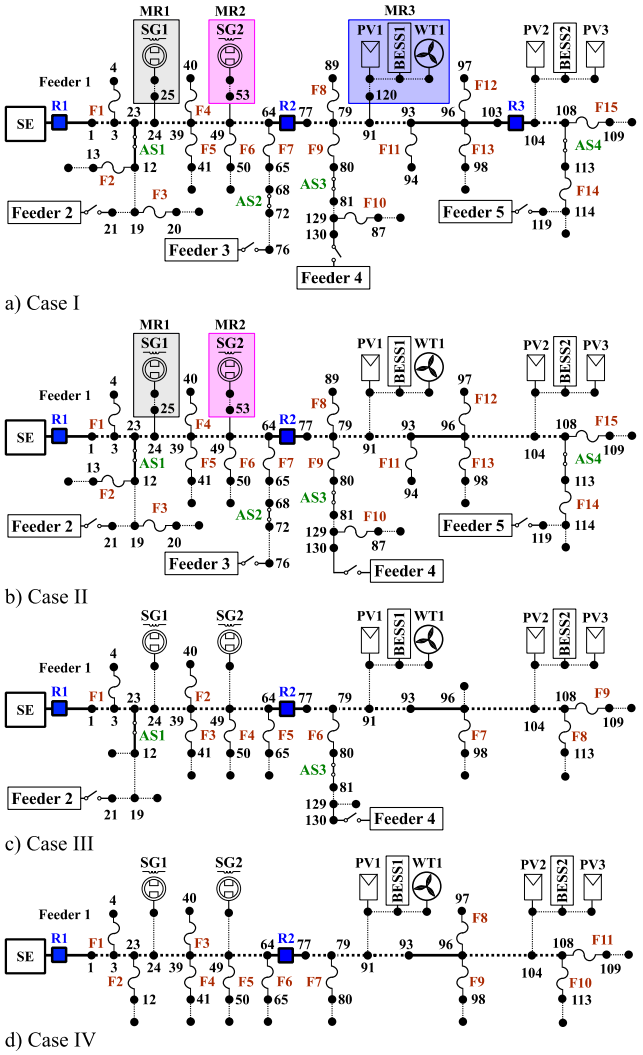

FIGURE 10. Case studies.

as branches 3-4 and 39-40. These allocations are strategic because a fault in such lines can compromise a significant portion of the distribution network.

Transferring loads to neighboring feeders using AS is an attractive strategy, with cases I, II, and III including such devices. In cases I and II, due to emphasis on CENS, all ASs allowed are installed. Feeders 2 and 4 are the preferred choice in most solutions from Pareto Front because of their higher capacity. In Case III, only feeders with higher capacity are allocated. In some solutions, line segments downstream ASs includes fuses to reduce the fault propagation, such as AS1 in cases I and II.

IID in microgrids supplied by renewable DG units represents 8% of Pareto Front solutions. However, this strategy has low attractiveness from the equipment cost point of view, including the compromise solutions in cases II, III, and IV. Thus, most solutions have no microgrids supplied by renewable DG.

The section with WT unit is the preferred choice in case I than the section with only PV units and BESS due to their higher total capacity and the possibility to operate in islanded mode in more scenarios. WT units present a better power output during the day concerning PV units, which can't produce energy at night. Besides, microgrid MG3 has a long line length and more loads than the section with only PV units and BESS. Such details can also provide more advantages in allocating an IID in WT unit region.

The proposal in case III comprises a good relation between both OF, being an interesting option for the decision-maker. The solution of cases I and II can be an interesting alternative depending on the period the company seeks the return on investment (ROI). The allocated devices last longer than the planning period established in the tests performed. Therefore, the equipment cost can be better spread over a more extended period. Moreover, the proposed method presents other solutions, allowing the decision-maker to choose the best solution based on the company's interest.

C. RESULTS CONSIDERING FIS

Estimating batteries' SoC using the OPF model provides a more realistic scenario regarding the island operation of microgrids supplied by renewable DG units and BESS. However, such a technique combined with the proposed method increases the computational response, leading a higher time to plan the protection system. Therefore, a FIS is also proposed to estimate the batteries' SoC.

Fig. 11 compares batteries' SoC between the OPF model and the FIS during seven days in January. The correlation coefficient is calculated to analyze the affinity between data provided by OPF model and FIS during the entire year. The higher the correlation coefficient, the greater the affinity between the data.

The FIS model uses the input parameters of demand, irradiation, wind speed, and energy price to predict the SoC. As shown in Fig. 11, such a technique provides similar results with a slight deviation. In some cases, the difference is higher because the input parameters present uncommon behavior regarding other days (see Sunday). However, the overall results are similar, presenting a strong affinity, with a correlation coefficient of 0.6826 [40].

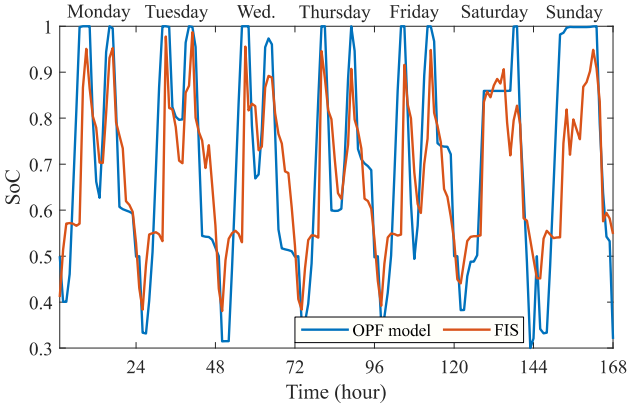

FIGURE 11. Comparison between batteries' SoC from OPF model and FIS.

Tests are performed again, changing batteries' SoC from OPF model to FIS. A comparison of Pareto Frontier from both methods is shown in Fig. 12. The k-means method reduces the scenarios using all data at the same time. Thus, the replacement of SoC data promotes a slight difference in time blocks and input parameters used in each technique, leading to changes in the CENS and equipment cost.

Fig. 13 shows a comparison between devices considered in Pareto Front solutions from both methods. Solutions with more than one recloser represent 54,33% of Pareto Front solutions against 61% using the OPF model. Solutions with at least one fuse also represent 99,67% of Pareto Front, while cases with the maximum number allowed are 14%, i.e., higher chances of allocating more fuses considering the FIS.

ASs are present in 77,67% of solutions compared to 80,33% using the OPF model. However, cases with the maximum number allowed are higher considering the FIS, with 28,33%. 43,66% of Pareto Front include IID, 0,44% less than using the OPF model. Cases with IID in microgrids supplied by renewable DG represent 4,33% of Pareto Front solutions compared to 4% using the OPF model. Thus, the FIS provides close conditions of islanded operation. Consequently, the solver finds similar solutions concerning the tests using the OPF model. The hypervolume using the FIS is 0.8721. Therefore, even with the difference in the input data, the results are similar, indicating that solving the optimal allocation problem using FIS also provides realistic results.

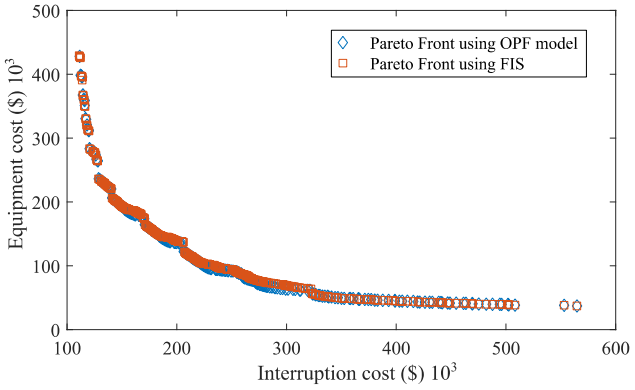

FIGURE 12. Pareto fronts from OPF model and FIS.

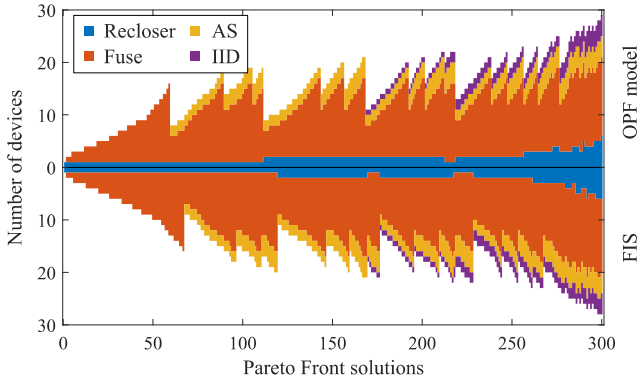

FIGURE 13. Comparison between pareto front solutions with the CENS in descending order.

V. CONCLUSION

This work proposes a method to solve the allocation problem of protection and control devices in distribution networks with microgrids. The NSGA-II solves the problem in a multiobjective approach, considering the CENS and equipment costs. The method includes the possibility of load transference and microgrids' island operation considering dispatchable and renewable DG and BESS. Besides, the proposal considers uncertainties parameters to provide more realistic results. A set of solutions is presented, highlighting the best compromise solution between OFs. These results allow the decision-maker to choose the best solution based on their interests.

Using a FIS to estimate de batteries' SoC also provides good results in solving the optimal allocation problem of protection and control devices. Thus, such a technique is an attractive option depending on how fast the decision-maker needs the results for planning the protection system.

This proposal determines the size and location of control and protection devices based on the distribution company's perspective. Include the customer damage function (CDF) to improve apart from other OFs could provide a more interesting setup. Also, it is assumed that coordination is possible in all solutions found. However, this is a feature that should be checked in future work.

Microgrids can be a promising strategy to improve continuity and reliability indices, as observed here and by related works cited in the literature review. Cases of microgrids supplied by renewable DG units present low attractiveness from the equipment cost point of view. This strategy may be more interesting, for example, if the reduction of CO_2 and NO_2 emissions have been considered an environmental restriction. Therefore, further studies must be carried out to evaluate the islanding operation of renewable DG units.

REFERENCES

[1] A. Bahmanyar, S. Jamali, A. Estebsari, and E. Bompard, "A comparison framework for distribution system outage and fault location methods," *Electr. Power Syst. Res.*, vol. 145, pp. 19–34, Apr. 2017, doi: 10.1016/j.epsr.2016.12.018.

[2] J. L. López-Prado, J. I. Vélez, and G. A. Garcia-Llinás, "Reliability evaluation in distribution networks with microgrids: Review and classification of the literature," *Energies*, vol. 13, no. 23, p. 6189, Nov. 2020, doi: 10.3390/en13236189.

[3] M. Soshinskaya, W. H. J. Crijns-Graus, J. M. Guerrero, and J. C. Vasquez, "Microgrids: Experiences, barriers and success factors," *Renew. Sustain. Energy Rev.*, vol. 40, pp. 659–672, Dec. 2014.

[4] J. Gouveia, C. Gouveia, J. Rodrigues, R. Bessa, A. G. Madureira, R. Pinto, C. L. Moreira, and J. A. Peças Lopes, "Microgrid energy balance management for emergency operation," in *Proc. IEEE Manchester PowerTech*, Jul. 2017, pp. 1–6, doi: 10.1109/PTC.2017.7981127.

[5] A. Abiri-Jahromi, M. Fotuhi-Firuzabad, M. Parvania, and M. Mosleh, "Optimized sectionalizing switch placement strategy in distribution systems," *IEEE Trans. Power Del.*, vol. 27, no. 1, pp. 362–370, Jan. 2012, doi: 10.1109/TPWRD.2011.2171060.

[6] L. S. de Assis, J. F. V. Gonzalez, F. L. Usberti, C. Lyra, C. Cavellucci, and F. J. Von Zuben, "Switch allocation problems in power distribution systems," *IEEE Trans. Power Syst.*, vol. 30, no. 1, pp. 246–253, Jan. 2015, doi: 10.1109/TPWRS.2014.2322811.

[7] J. de La Barra, E. Gil, A. Angulo, and A. Navarro-Espinosa, "Effect of failure rates uncertainty on distribution systems reliability," in *Proc. IEEE Power Energy Soc. General Meeting*, Aug. 2020, pp. 1–5, doi: 10.1109/PESGM41954.2020.9281459.

[8] E. Zambon, D. Z. Bossois, B. B. Garcia, and E. F. Azeredo, "A novel nonlinear programming model for distribution protection optimization," *IEEE Trans. Power Del.*, vol. 24, no. 4, pp. 1951–1958, Oct. 2009, doi: 10.1109/TPWRD.2008.2002679.

[9] G. A. G. Mercado and J. W. G. Sanchez, "Optimization of reclosers placement in distribution networks to improve service quality indices," *IEEE Latin Amer. Trans.*, vol. 20, no. 2, pp. 241–249, Feb. 2022, doi: 10.1109/TLA.2022.9661463.

[10] K. D. McBee, I. Fareez, and C. Pardington, "Identifying DA allocation by minimizing the overall cost of customer minutes interrupted," *IEEE Trans. Power Del.*, vol. 36, no. 3, pp. 1694–1704, Jun. 2021, doi: 10.1109/TPWRD.2020.3013233.

[11] A. V. Pombo, J. Murta-Pina, and V. F. Pires, "Multiobjective planning of distribution networks incorporating switches and protective devices using a memetic optimization," *Rel. Eng. Syst. Saf.*, vol. 136, pp. 101–108, Apr. 2015, doi: 10.1016/j.ress.2014.11.016.

[12] J.-M. Sohn, S.-R. Nam, and J.-K. Park, "Value-based radial distribution system reliability optimization," *IEEE Trans. Power Syst.*, vol. 21, no. 2, pp. 941–947, May 2006, doi: 10.1109/TPWRS.2005.860927.

[13] L. G. W. da Silva, R. A. F. Pereira, and J. R. S. Mantovani, "Allocation of protective devices in distribution circuits using nonlinear programming models and genetic algorithms," *Electr. Power Syst. Res.*, vol. 69, no. 1, pp. 77–84, 2004, doi: 10.1016/j.epsr.2003.08.010.

[14] W. Tippachon and D. Rerkpreedapong, "Multiobjective optimal placement of switches and protective devices in electric power distribution systems using ant colony optimization," *Electr. Power Syst. Res.*, vol. 79, no. 7, pp. 1171–1178, Jul. 2009, doi: 10.1016/j.epsr.2009.02.006.

[15] M. Izadi, A. Safdarian, M. Moeini-Aghtaie, and M. Lehtonen, "Optimal placement of protective and controlling devices in electric power distribution systems: A MIP model," *IEEE Access*, vol. 7, pp. 122827–122837, 2019, doi: 10.1109/ACCESS.2019.2938193.

[16] M. M. Costa, M. Bessani, and L. Batista, "A multiobjective and multicriteria approach for optimal placement of protective devices and switches in distribution networks," *IEEE Trans. Power Del.*, early access, Oct. 19, 2021, doi: 10.1109/TPWRD.2021.3120968.

[17] Ž. Popović, B. Brbaklić, and S. Knežević, "A mixed integer linear programming based approach for optimal placement of different types of automation devices in distribution networks," *Electr. Power Syst. Res.*, vol. 148, pp. 136–146, Jul. 2017, doi: 10.1016/j.epsr.2017.03.028.

[18] A. Alam, M. Tariq, M. Zaid, P. Verma, M. Alsultan, S. Ahmad, A. Sarwar, and M. A. Hossain, "Optimal placement of reclosers in a radial distribution system for reliability improvement," *Electronics*, vol. 10, no. 24, p. 3182, Dec. 2021, doi: 10.3390/electronics10243182.

[19] V. Calderaro, V. Lattarulo, A. Piccolo, and P. Siano, "Optimal switch placement by alliance algorithm for improving microgrids reliability," *IEEE Trans. Ind. Informat.*, vol. 8, no. 4, pp. 925–934, Nov. 2012, doi: 10.1109/TII.2012.2210722.

[20] C. A. P. Meneses and J. R. S. Mantovani, "Improving the grid operation and reliability cost of distribution systems with dispersed generation," *IEEE Trans. Power Syst.*, vol. 28, no. 3, pp. 2485–2496, Aug. 2013, doi: 10.1109/TPWRS.2012.2235863.

[21] K. Pereira, B. R. Pereira, J. Contreras, and J. R. S. Mantovani, "A multiobjective optimization technique to develop protection systems of distribution networks with distributed generation," *IEEE Trans. Power Syst.*, vol. 33, no. 6, pp. 7064–7075, Nov. 2018, doi: 10.1109/TPWRS.2018.2842648.

[22] H. Karimi, T. Niknam, M. Dehghani, M. Ghiasi, M. Ghasemigarpachi, S. Padmanaban, S. Tabatabaee, and H. Aliev, "Automated distribution networks reliability optimization in the presence of DG units considering probability customer interruption: A practical case study," *IEEE Access*, vol. 9, pp. 98490–98505, 2021, doi: 10.1109/ACCESS.2021.3096128.

[23] A. Heidari, V. G. Agelidis, M. Kia, J. Pou, J. Aghaei, M. Shafie-Khah, and J. P. S. Catalão, "Reliability optimization of automated distribution networks with probability customer interruption cost model in the presence of DG units," *IEEE Trans. Smart Grid*, vol. 8, no. 1, pp. 305–315, Jan. 2017.

[24] M. Lwin, J. Guo, N. Dimitrov, and S. Santoso, "Protective device and switch allocation for reliability optimization with distributed generators," *IEEE Trans. Sustain. Energy*, vol. 10, no. 1, pp. 449–458, Jan. 2019, doi: 10.1109/TSTE.2018.2850805.

[25] W. R. Faria, C. A. L. Nametala, and B. R. Pereira, "Cost-effectiveness enhancement in distribution networks protection system planning," *IEEE Trans. Power Del.*, vol. 8977, no. 2, pp. 1–12, Apr. 2021, doi: 10.1109/TPWRD.2021.3079926.

[26] A. Alam, V. Pant, and B. Das, "Optimal placement of protective devices and switches in a radial distribution system with distributed generation," *IET Gener., Transmiss. Distrib.*, vol. 14, no. 21, pp. 4847–4858, Nov. 2020, doi: 10.1049/iet-gtd.2019.1945.

[27] T. D. de Lima, A. Tabares, N. Bañol Arias, and J. F. Franco, "Investment generation costs vs CO_2 emissions in the distribution system expansion planning: A multi-objective stochastic programming approach," *Int. J. Electr. Power Energy Syst.*, vol. 131, Oct. 2021, Art. no. 106925, doi: 10.1016/j.ijepes.2021.106925.

[28] M. S. Javadi, R. Azami, and H. Monsef, "Security constrained unit commitment of interconnected power systems," *Int. Rev. Elect. Eng.*, vol. 4, no. 2, pp. 199–205, 2009.

[29] M. S. Javadi, M. Lotfi, M. Gough, A. E. Nezhad, S. F. Santos, and J. P. S. Catalao, "Optimal spinning reserve allocation in presence of electrical storage and renewable energy sources," in *Proc. IEEE Int. Conf. Environ. Electr. Eng. IEEE Ind. Commercial Power Syst. Eur. (EEEIC/ICPS Europe)*, Jun. 2019, pp. 1–6, doi: 10.1109/EEEIC.2019.8783696.

[30] Mathworks. *MATLAB 2017*. Accessed: Mar. 7, 2021. [Online]. Available: https://www.mathworks.com

[31] K. Deb, A. Pratap, S. Agarwal, and T. Meyarivan, "A fast and elitist multiobjective genetic algorithm: NSGA-II," *IEEE Trans. Evol. Comput.*, vol. 6, no. 2, pp. 182–197, Apr. 2002, doi: 10.1109/4235.996017.

[32] S. Kannan, S. Baskar, J. D. McCalley, and P. Murugan, "Application of NSGA-II algorithm to generation expansion planning," *IEEE Trans. Power Syst.*, vol. 24, no. 1, pp. 454–461, Feb. 2009, doi: 10.1109/TPWRS.2008.2004737.

[33] N. Srinivas and K. Deb, "Muiltiobjective optimization using nondominated sorting in genetic algorithms," *J. Evol. Comput.*, vol. 2, no. 3, pp. 221–248, Sep. 1994, doi: 10.1162/evco.1994.2.3.221.

[34] M. A. Alotaibi and M. M. A. Salama, "An incentive-based multistage expansion planning model for smart distribution systems," *IEEE Trans. Power Syst.*, vol. 33, no. 5, pp. 5469–5485, Sep. 2018, doi: 10.1109/TPWRS.2018.2805322.

[35] S. Pfenninger and I. Staffell. (Mar. 6, 2021). *Renewable.ninja—Simulations of the Hourly Power Output From Wind and Solar Power Plants*. Accessed: Mar. 5, 2021. [Online]. Available: https://www.renewables.ninja/

[36] Redes Energéticas Nacionais (REN). *Balanço Energético—REN Data Hub*. Accessed: Dec. 23, 2021. [Online]. Available: https://datahub.ren.pt/pt/eletricidade

[37] OMIE. *Iberian Market Operator—Portuguese Branch (OMIE)*. Accessed: Dec. 23, 2021. [Online]. Available: https://www.omie.es/pt/file-access-list

[38] A. P. Guerreiro, C. M. Fonseca, and L. Paquete, "The hypervolume indicator: Computational problems and algorithms," *ACM Comput. Surv.*, vol. 54, no. 6, pp. 1–42, Jul. 2021, doi: 10.1145/3453474.

[39] S. F. Adra, T. J. Dodd, I. A. Griffin, and P. J. Fleming, "Convergence acceleration operator for multiobjective optimization," *IEEE Trans. Evol. Comput.*, vol. 13, no. 4, pp. 825–847, Aug. 2009, doi: 10.1109/TEVC.2008.2011743.

[40] J. Ramsebner, P. Linares, and R. Haas, "Estimating storage needs for renewables in Europe: The correlation between renewable energy sources and heating and cooling demand," *Smart Energy*, vol. 3, Aug. 2021, Art. no. 100038, doi: 10.1016/j.segy.2021.100038.

CLEBERTON REIZ (Graduate Student Member, IEEE) received the B.Sc. degree in electrical engineering from Mato Grosso State University (UNEMAT), Sinop, Brazil, in 2017, and the M.Sc. degree in electrical engineering from São Paulo State University (UNESP), Ilha Solteira, Brazil, in 2019, where he is currently pursuing the Ph.D. degree. Since 2021, he has been a Visiting Student with the Institute for Systems and Computer Engineering, Technology and Science (INESC TEC), Porto, Portugal. His current research interests include the development of methods for the optimization, planning, and control of electrical power systems.

TAYENNE DIAS DE LIMA (Graduate Student Member, IEEE) received the B.Sc. degree in electrical engineering from Mato Grosso State University, Sinop, Brazil, in 2017, and the M.Sc. degree in electrical engineering from São Paulo State University, Ilha Solteira, Brazil, in 2019, where she is currently pursuing the Ph.D. degree in electrical engineering. Her current research interests include methods for the optimization of power systems and distribution systems expansion planning.

JONATAS BOAS LEITE (Member, IEEE) received the B.Sc. and Ph.D. degrees in electrical engineering from Sao Paulo State University (UNESP), Ilha Solteira, Brazil, in 2010 and 2015, respectively. He was a Postdoctoral Researcher with the Electrical and Computer Engineering Department, Texas A&M University, College Station, TX, USA, and the Electrical Engineering Postgraduate Program of UNESP, in 2016 and 2019, respectively. He is currently a Professor with the Department of Electrical Engineering, UNESP, and the Laboratorio de Planejamento de Sistemas de Energia Eletrica, Ilha Solteira. His research interest includes planning and control of electrical power systems.

MOHAMMAD SADEGH JAVADI (Senior Member, IEEE) received the B.Sc. degree from Shahid Chamran University, Ahwaz, Iran, in 2007, the M.Sc. degree in power system from the University of Tehran, in 2009, and the Ph.D. degree in electrical power engineering from Shahid Chamran University, in 2014. He is currently an Associate Professor at IAU, Shiraz, Iran, and also a Researcher at the INESC TEC, Porto, Portugal. His research interests include power system operations and planning, multi-carrier energy systems, islanding operation of active distribution networks, distributed renewable generation, demand response, and smart grid. He received the Best Reviewer Awards from the IEEE TRANSACTIONS ON SMART GRID and the IEEE TRANSACTIONS ON POWER SYSTEM in 2019. Since 2021, he has been serving as an Associate Editor for *e-Prime* journal.

CLARA SOFIA GOUVEIA received the M.Sc. and Ph.D. degrees in electrical engineering from the Faculty of Engineering, University of Porto (FEUP), in 2008 and 2015, respectively. She has been a member of the Centre for Power and Energy Systems, INESC TEC, since 2011, currently a Senior Researcher. She is also leading the Center EMS/DMS and network automation area. She has been involved in several national and European projects, such as MERGE, SENSIBLE, and UPGRID Project, namely in the development and demonstration activities in INESC TEC Smart Grids and Electric Vehicles Laboratory of control and management strategies to enable the safe integration of distributed energy resources in distribution networks, particularly when operating islanded from the main grid. Her research interests include the operation of distribution networks within smart grid context, considering the large-scale integration of distributed energy resources and microgrid concepts.